PLASMA ASSISTED NITRIDING OF TEMPERED AND AS-QUENCHED AISI420 MARTENSITIC STAINLESS STEEL AT LOW TEMPERATURE

Fernando Irto Zanetti, fizanetti@msn.com
Thiago Fernandes Amaral, thiagofamaral@hotmail.com
Rodrigo Perito Cardoso, rodrigo.perito@ufpr.br
Cristiano José Scheuer, cristiano.scheuer@ufpr.br
Sílvio Francisco Brunatto, brunatto@ufpr.br
Universidade Federal do Paraná (UFPR), Av. Cel. Francisco H. dos Santos, 210 - Curitiba/PR – Brasil

Abstract. *AISI 420 stainless steel is commonly applied when high strength and corrosion resistance are needed. This steel stands out by the possibility of thermal and/or thermochemical treatments, such as quenching and nitriding. The nitriding main purpose is the improvement of tribological properties of the material by forming a surface layer of nitrides and/or by forming a diffusion layer of nitrogen, in interstitial form, increasing the surface hardness. A limiting factor for the nitriding of stainless steel is the treatment temperature, which can lead to a decrease of chromium content in solid solution near the surface by chromium nitrides precipitation, leading to a reduced corrosion resistance. However, the plasma assisted nitriding process distinguishes itself by allowing performing the treatment at sufficiently low temperatures. Moreover, the process has also high treatment efficiency with high operational and environmental safety, being generally non-polluting. In the present work, the microstructural evolution of samples is investigated for different treatment temperatures. Samples were made of AISI 420 martensitic stainless steel on as-quenched and tempered state. The microstructural evolution is studied by metallographic examination of cross-sectioned samples by optical microscopy, micro-hardness test and X-ray diffraction. The results indicate that treatment temperature is a determining factor for the thickness of hardened layer and also for the precipitation of chromium nitrides. The apparent surface hardness is directly affected by the thickness of hardened layer, by its hardness and by the microstructure of the bulk material.*

Keywords*: Plasma Assisted Nitriding, Low Temperature Plasma Assisted Nitriding, AISI 420 Steel, Nitriding Kinetics.*

1. INTRODUCTION

The AISI 420 martensitic stainless steel is widely applied when mechanical strength and high corrosion resistance are needed (Figueroa *et al.* (2005), Isfahany *et al.* (2011), Kim, *et al.* (2003)). However, its low wear resistance can limit its application (Alphonsa *et al.* (2002), Pinedo and Monteiro, (2004)), and thus, it is necessary to improve the surface characteristics of this materials. So in recent decades, researches were conducted with the aim of improving its wear and corrosion resistance, through the application of plasma assisted technology (Zhang and Bell, 1985; Ichii *et al.,* 1986; Davis, 1994; Menthe *et al*., 1995). Among plasma assisted techniques, the nitriding have shown good results in practical applications and have demanded the attention of researchers in the metallurgical-mechanical field (Alphonsa *et al.* (2002), Pinedo and Monteiro, 2004, Kim, *et al.* (2003), Xi *et al*. (2008)[a], Xi *et al*. (2008)[b]). However, when this treatment is performed at high temperatures, it can also lead to a drastic reduction in corrosion resistance due to formation of chromium nitrides, lowering the concentration of chromium in solid solution, when the temperature exceeds 723 K (Li and Bell, 2004). Nevertheless, when the plasma nitriding treatment is carried out at temperature, below 723 K, the obtained modified layer consists of a nitrogen supersaturated phase known as expanded martensite (a_N), which presents high hardness, wear resistance and corrosion resistance (Kim *et al.* 2003).

Based on the above, in the present work it was studied the AISI 420 martensitic stainless steel plasma assisted nitriding treatment. Whereas several studies have been conducted for martensitic stainless steels nitriding, but there are few studies of the effect of the tempering state (associated to stress state and defect density) on the nitriding layer properties and on the nitriding kinetics. So, this study aims to verify the influence of tempering state both in the layer thickness and in the obtained surface hardness, for as-quenched and tempered AISI420 samples.

2. EXPERIMENTAL PROCEDURES

2.1. Treatment

The nitriding chamber consists of a stainless steel cylinder with 350 mm in diameter and 380 mm in height, closed and supported by stainless steel plates of 360 mm in diameter sealed by O-rings. The sample holder of 50.8 mm diameter and 10 mm high acted as the cathode of the glow discharge. It contains four 10 mm holes arranged with radial symmetry to hold the specimens, which are also part of the cathode (Fig. 1). The pressure inside the chamber was measured by a capacitive manometer of 1.33 x 10^4 Pa full-scale, being regulated by a manual valve. The temperature

was measured by a chromel-alumel (K-type) thermocouple with 1.5 mm diameter and it was controlled by the swished-on time of the pulsed power supply. The gas flow rate and composition was regulated by 3 mass flow controllers.

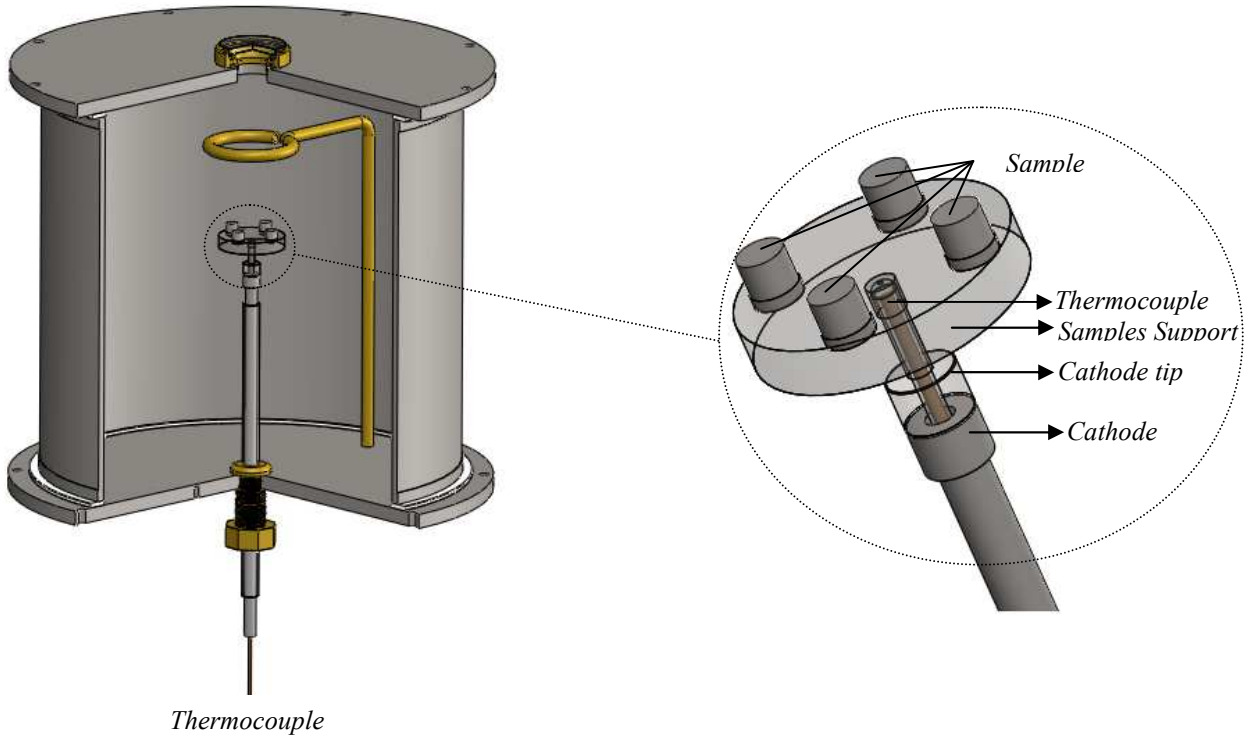

Figure 1. Schematic representation of the vacuum chamber and of the sample support configuration applied in the plasma assisted low temperature nitriding treatment

Cylindrical samples 15 mm height were obtained from a commercial rod of diameter 9.5 mm. The material was austenitized at 1323 K (1050 ºC) for thirty minutes, followed by air quenching. The tempered samples were heated up until 673 K (400 ºC) for an hour. After quenching or tempering the samples were fine ground and polished with 1 µm alumina and alcohol cleaned before treatment.

The samples were placed on the support (as shown in fig. 1) and the vacuum chamber was pumped down to a residual pressure of 1.33 Pa. After achieving the residual pressure, H_2 was introduced in order to flush the system. The process was repeated three times with the purpose to remove any impurities from the vacuum chamber. After flushing, the gas flow, composed of a mixture of 90% H_2 + 10% Ar, was set to 200 sccm (standard cubic centimeter per minute). So the pressure of 400 Pa was adjusted by the manual valve for the cleaning step. A power supply peak voltage of 600 V with a pulse period of 240 µs was applied to generate the plasma and the samples were sputter-cleaned for 1.8×10^3 s (0.5 h) at a temperature of 573 K.

After cleaning, the gas flow was maintained constant and the gas mixture was modified to 70% N_2 + 20% H_2 + 10% Ar. The nitriding treatments were performed at temperatures of 573 K, 623 K, 673 K and 723 K (300, 350, 400 and 450 ºC, respectively). After treatment, samples were cooled down under the same gas flow down to the room temperature.

2.2. Samples characterization

The samples were first characterized by X-ray diffraction using a Shimadzu XDR7000 x-ray diffractometer with a Cu *Kα* X-ray tube. The 2θ angle was scanned from 30° to 90° at the speed of 1 deg/min in steps of 0.02°. After the X-ray diffraction measurements, the surface hardness was measured with a Shimadzu Micro Hardness Tester HMV-2T, applying a load of 300 gf for a peak-load contact of 15 s. So, samples were cross sectioned, metallographic prepared and the treated layer thickness and microstructure were analyzed. For microstructural analysis, samples were etched with the chemical reagent Villela (50 ml HCl and 10 g of picric acid in 1000 ml alcohol) and analyzed by Olympus BX51M optical microscope.

3. RESULTS AND DISCUSSION

3.1. Surface Hardness

Hardness test results are depicted in Fig. 2. Before treatment the harness of as-quenched and tempered samples were 408 $HV_{0.3}$ and 350 $HV_{0.3}$, respectively. An increase on surface hardness with the treatment temperature is observed, reaching 1652 $HV_{0.3}$ for the as-quenched sample and 1139 $HV_{0.3}$ for the tempered samples. It is worth mentioning that the microhardness measurements were performed with a load of 300 gf, which represents a significant value. It is to be noted that the measured surface hardness is not the actual layer hardness but an apparent hardness, since the penetration depth can be of the same order of the layer thickness. So its value is dependent on the layer hardness, on the layer thickness and on the bulk material hardness. Insomuch the increase in the surface hardness from 573 to 723 K can be attributed not only for the increase in the nitrogen content in the related layer but alto to the increase of the layer thickness.

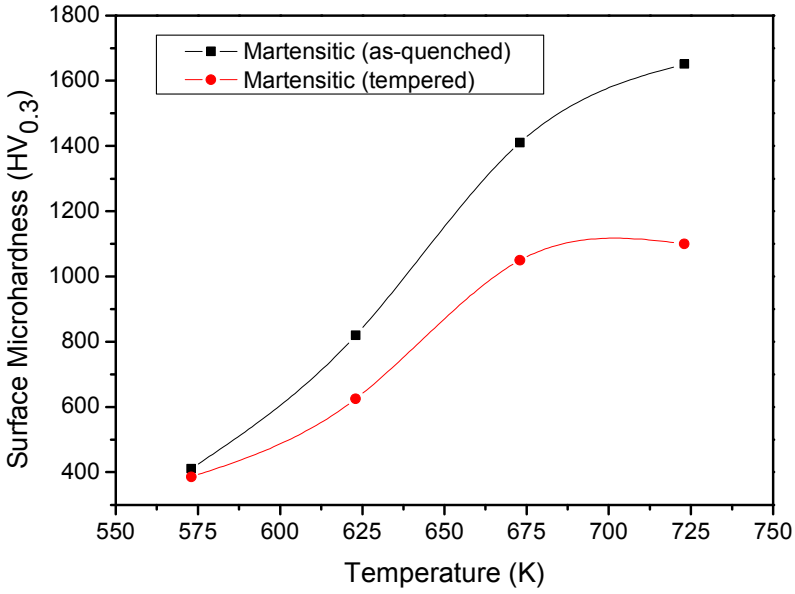

Figure 2. Surface hardness as a function of nitriding temperature. Samples treated for 4 h at a gas mixture composition 70% N_2 + 20% H_2 + 10% Ar and flow of 200 sccm at pressure of 3 torr

3.2. Metallographic analysis

Optical micrographs of cross-sectioned treated samples are present in Fig. 3 and Fig. 4, for as-quenched and tempered samples respectively. The metallographic analysis showed the presence of a modified layer on the sample surface for all studied temperatures. For samples treated at 723 K, Fig. 3(d) and Fig. 4(d) the corrosion (etch) of parts of the nitrided layer can be observed, it is due to localized attack caused by the chromium nitrides precipitation at grain boundaries causing a local drop in corrosion resistance. It can also be observed that the treated layer is slightly thinner in the tempered sample. This fact is attributed to the lower internal stress and lower density of defects in the crystal lattice of tempered samples, which are in fact high diffusion path. So, the diffusion coefficient of nitrogen into the matrix is higher for as-quenched samples. Comparing as-quenched and tempered samples it can be observed that the precipitation of nitrides is more effective for tempered samples.

By the micrographs it can be also observed that the nitrogen-rich layers are more resistant to the etchant (Villela), especially for low treatment temperatures, indicating that the treated layer presents higher corrosion resistance if compared to bulk material when no chromium nitride is precipitated.

In Fig. 5 the evolution of the carburized layer thickness as a function of the temperature treatment is shown. It may be noted that the parameter temperature can enhance thickness of the plasma nitride layer. The obtained thicknesses were 5.82, 10.88, 14.87 and 41.61, and 2.84, 6.41, 11.85 and 36.48 to as-quenched and tempered condition, respectively. These results demonstrate both that temperature plays an important role on the extent of the compound layer, but also the conditioning of samples by thermal treatment. Since there is considerable variation between the thickness of the layers of compounds obtained for the as-quenched and tempered conditions.

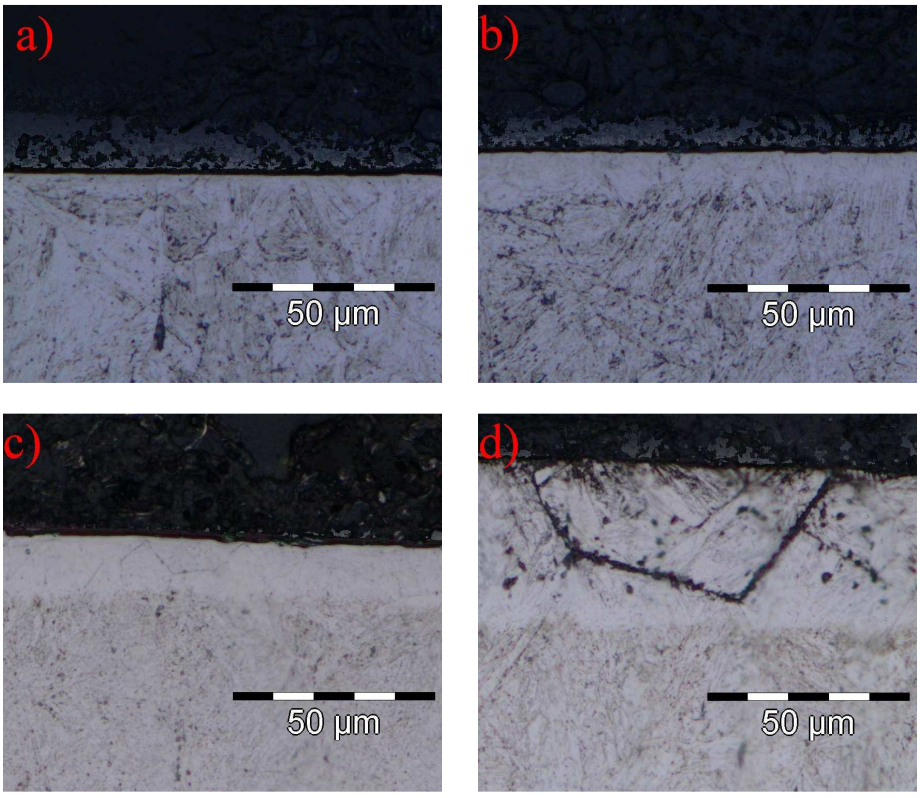

Figure 3. Optical micrographs of as-quenched samples at: a) 573 K, b) 623 K, c) 673 K and d) 723 K. Samples treated for 4 h at a gas mixture composition 70% N_2 + 20% H_2 + 10% Ar and flow of 200 sccm at pressure of 3 torr

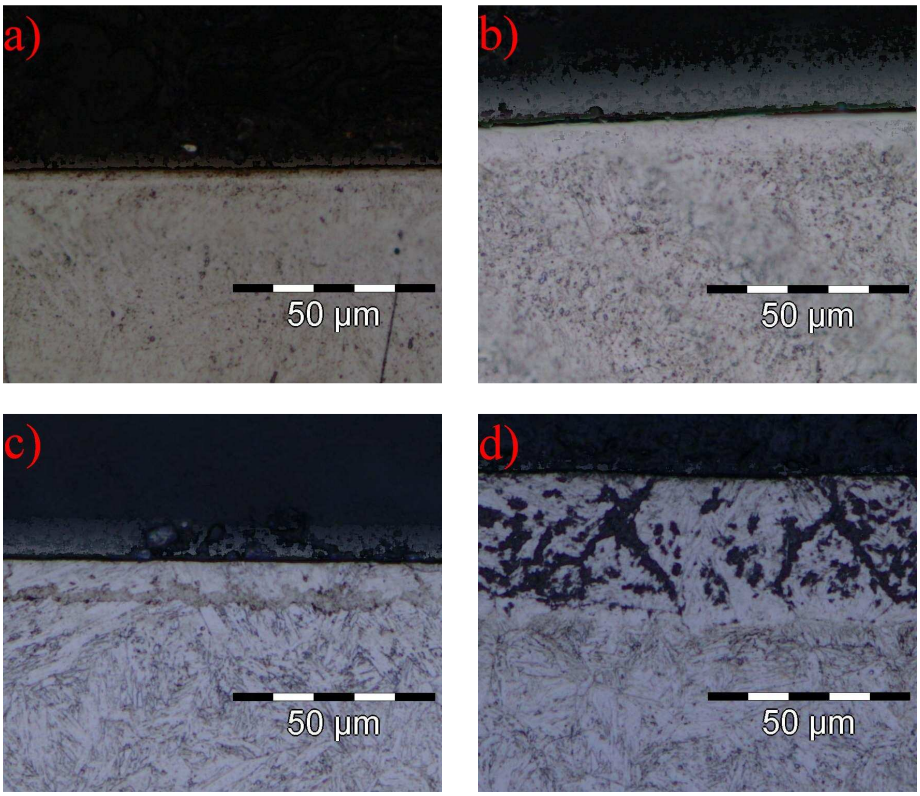

Figure 4. Optical micrographs of tempered samples nitride at: a) 573 K, b) 623 K, c) 673 K and d) 723 K. Samples treated for 4 h at a gas mixture composition 70% N_2 + 20% H_2 + 10% Ar and flow of 200 sccm at pressure of 3 torr

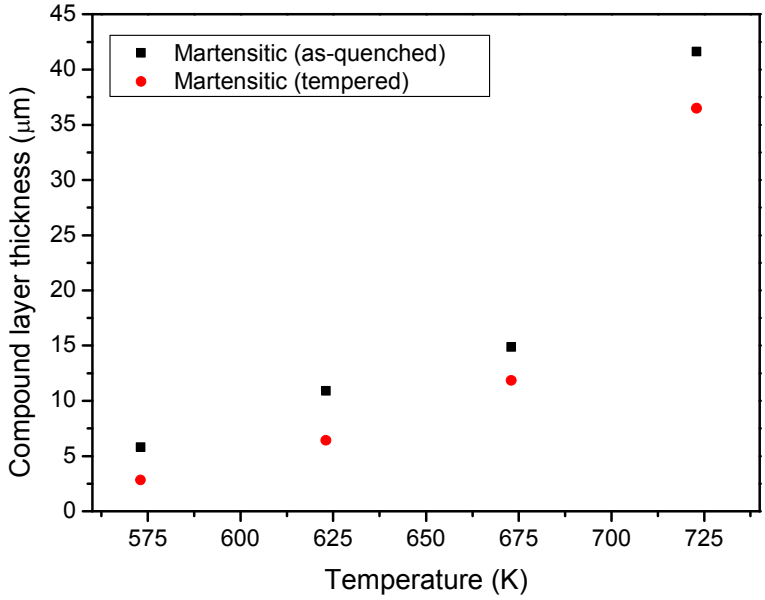

Figure 5. Evolution of the compound layer thickness as a function of treatment temperature. Samples treated for 4 h at a gas mixture composition 70% N_2 + 20% H_2 + 10% Ar and flow of 200 sccm at pressure of 3 torr

From the values of thickness of the compound present in the Fig. 5, one can calculate the activation energy for diffusion of nitrogen (Qd) by Arrhenius plot. The Arrhenius plot of the layer thickness is presents in Fig. 6, by this figure it possible to obtain the activation energy for nitrogen diffusion by the linearization presented in Eq. (1). It is proportional to the slope of the curve. By analyzing Fig. 6, it is expected that the activation energy is approximately the same for both samples at high temperature, but, at low temperature, a lower activation energy is expected for as-quenched samples, being an indication of high importance of high diffusion path (probably diffusion pipes). This can be attributed to the high defect density in the as-quenched state when compared to the termed state.

$$ln\, d = cte - \frac{Q_d}{2RT} \tag{1}$$

Where:
d is the layer thickness,
Q_d is the activation energy for diffusion (J/mol),
R is the gas constant (8,31 J/mol-K) and
T is the absolute temperature (K).

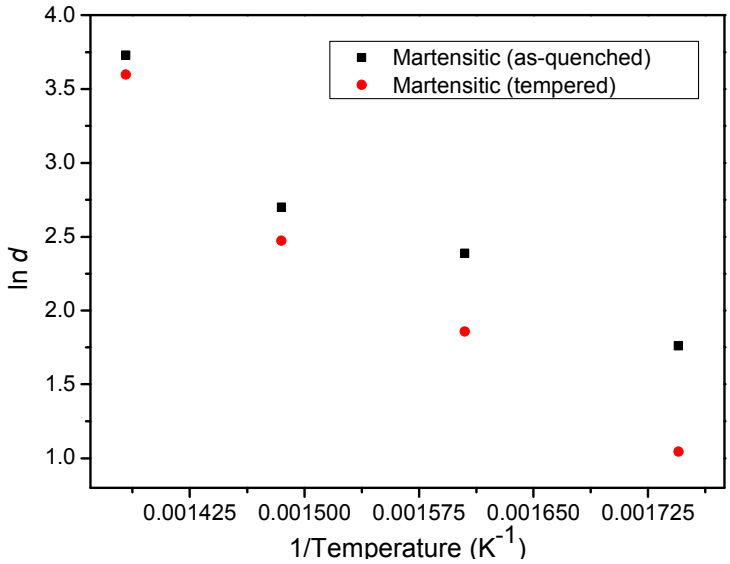

Figure 6. Arrhenius plot of the layer thickness. Determination of the activation energy for nitrogen diffusion. Samples treated for 4 h at a gas mixture composition 70% N_2 + 20% H_2 + 10% Ar and flow of 200 sccm and pressure of 3 torr

3.3. X-Ray Diffraction

The diffraction pattern presented in Fig. 7 was obtained from an untreated sample and shows only peaks of α-Fe (110, 200 and 211 respectively) in the studied angle range of 30°–90°.

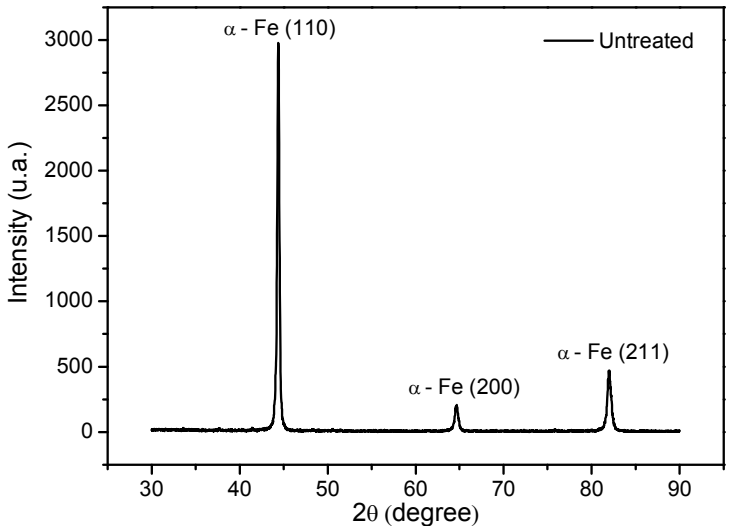

Figure 7. Diffraction pattern of the untreated AISI 420 sample. It is in the annealed condition with ferritic structure

The diffraction pattern presented in Fig. 8 was obtained from an as-quenched nitrided sample, showing peaks of ε iron nitride and expanded martensite (α_N). The α_N phase is characterized by a slightly shift of α-Fe peak to the left, indicating an expansion of the lattice due to the super-saturation of martensite with nitrogen, generating a microstructure called expanded martensite.

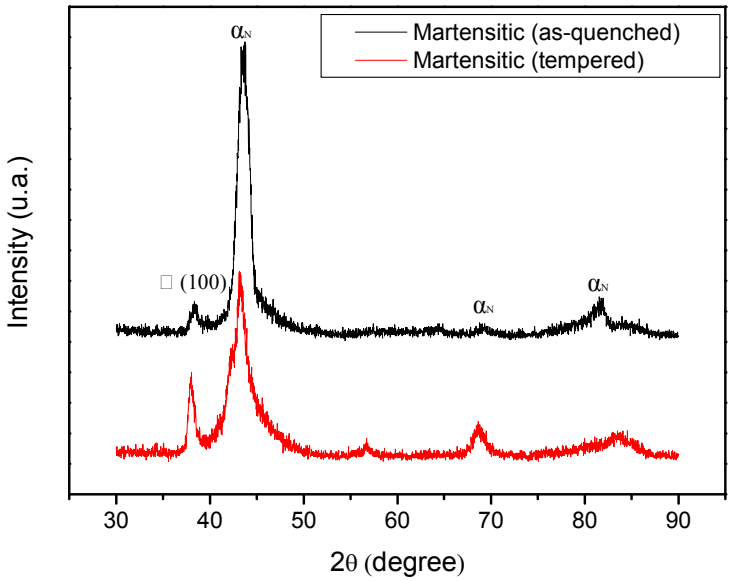

Figure 8. Diffraction pattern for as-quenched sample nitrided at 573 K. Samples treated for 4 h at a gas mixture composition 70% N_2 + 20% H_2 + 10% Ar and flow of 200 sccm at pressure of 3 torr

The diffraction patterns shown in Fig. 9 and Fig. 10 were obtained from samples nitrided at 623 K and 673 K, respectively. Their surfaces are composed of ε iron nitrides and expanded martensite (α_n), being the ε iron nitrides probably the dominating phase.

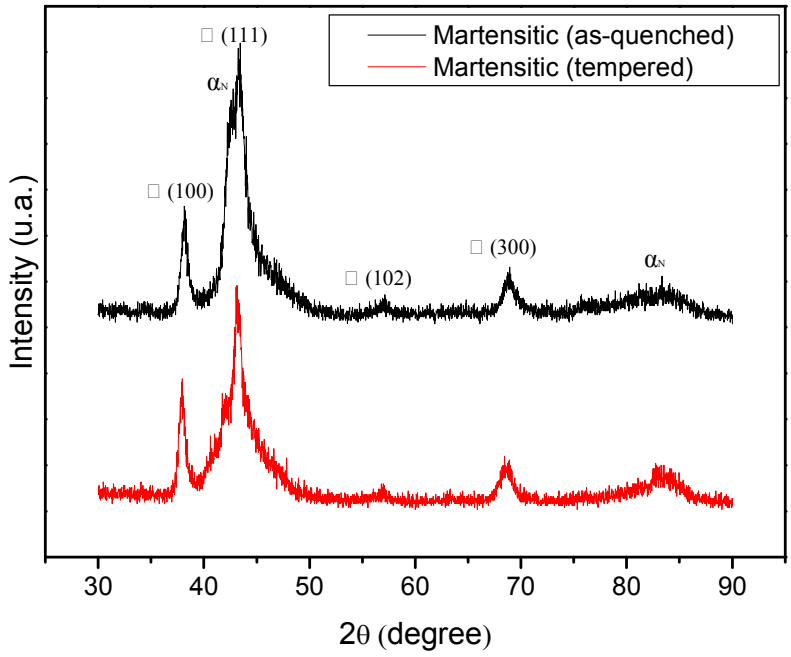

Figure 9. Diffraction patterns for as-quenched sample nitrided at: 623 K. Samples treated for 4 h at a gas mixture composition 70% N_2 + 20% H_2 + 10% Ar and flow of 200 sccm at pressure of 3 torr

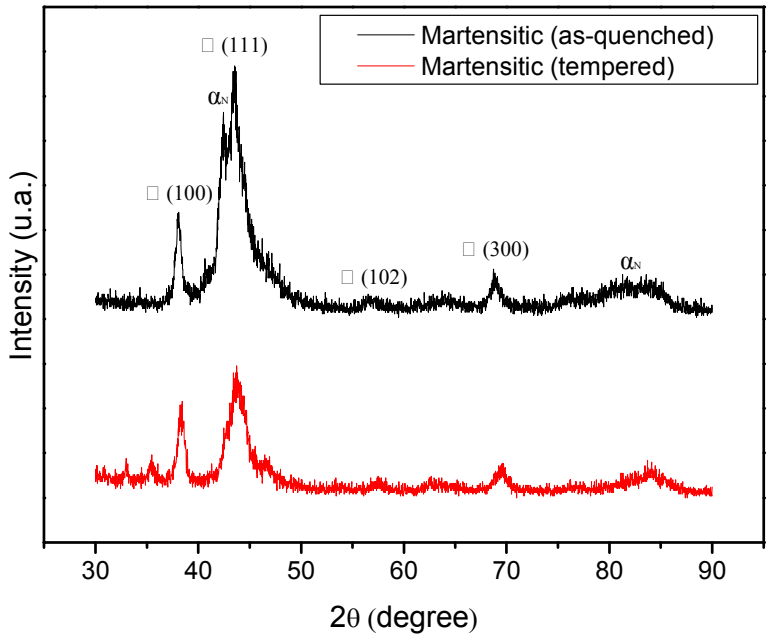

Figure 10. Diffraction patterns for as-quenched sample nitrided at 673 K. Samples treated for 4 h at a gas mixture composition 70% N_2 + 20% H_2 + 10% Ar and flow of 200 sccm at pressure of 3 torr.

The diffraction pattern of the as-quenched sample nitrided at 723K is presented in Fig. 11. It reveals that it is composed of ε iron nitrides, expanded martensite (α_N), chromium nitride (CrN) and iron nitride (Fe_3N). The presence of peaks of chromium nitrides (CrN) could be expected due to increased chromium mobility at this temperature, agreeing to the observed microstructure (Fig. 3(d) and Fig. 4(d)). The peaks of α_N could not be accurately determined since they were overlapped by the peaks of CrN and ε.

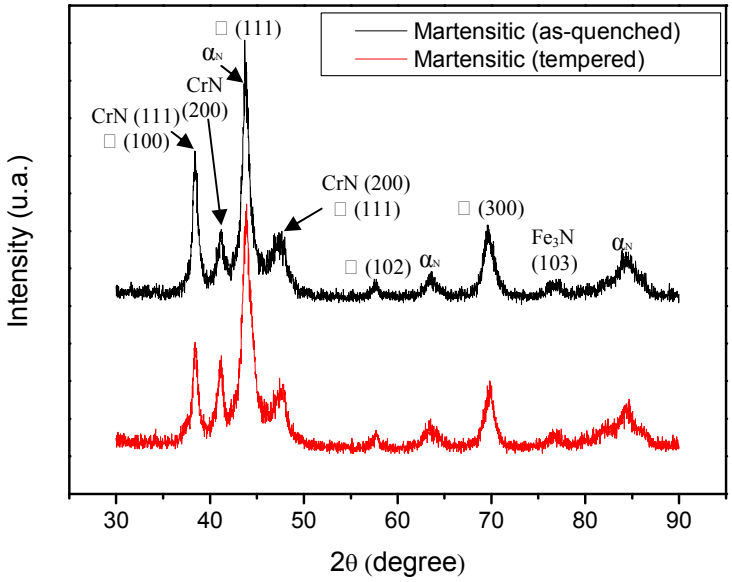

Figure 11. Diffraction pattern for as-quenched sample nitrided at 723 K. Samples treated for 4 h at a gas mixture composition 70% N_2 + 20% H_2 + 10% Ar and flow of 200 sccm at pressure of 3 torr.

4. CONCLUSIONS

From the presented results it can be concluded that the tempering state plays an important role on the nitriding kinetics on the AISI420 satin less steel. The following specific conclusions can be drawn:

a) The surface hardness of stainless steels can be strongly increased by nitriding treatment, with higher limit of about $1600HV_{0.3}$, in the studied conditions, over a substrate with just $400HV_{0.3}$.
b) The surface hardness of the as-quenched nitrided samples remained superior to the tempered samples, probably due to higher content of nitrogen into the treated layer, but it could also be due to higher hardness of the substrate and to the modified layer thickness.
c) The thickness of the treated layer, specially at low temperature, is higher for the as-quenched samples, presenting lower activation energy for nitrogen diffusion, what is attributed to the higher defect density of as-quenched samples.
d) Even if rapid layer growth can be obtained at high temperatures, it leads to precipitation of chromium nitrides, leading to a strong reduction of AISI420 corrosion resistance.

5. ACKNOWLEDGEMENTS

The authors would like to gratefully acknowledge the Brazilian Coordination Agency for Improvement of Higher Personnel – CNPq, for financial support to research (scholarship) that resulted in this work. The authors wish to express their thanks to the Laboratory of X-ray optics and Instrumentation – LORXI, from the *Universidade Federal do Paraná* – UFPR by the use of X-ray diffraction equipment.

6. REFERENCES

Alphonsa, I., Chainani, A., Raole, P.M., Ganguli B., John, P.I., A study of martensitic stainless steel AISI 420 modified using plasma nitriding. Surface and Coatings Technology 150 (2002) 263–268.

Davis, J.R., 1994, ASM Handbook, vol. 5, ASM International, Materials Park, Ohio, pp. 741–761.

Figueroa, C.A., Alvarez, F., Zhang, Z., Collins, G.A., Short, K.T., Structural modifications and corrosion behavior of martensitic stainless steel nitrided by plasma immersion ion implantation, J. Vac. Sci. Technol. A, Vol.23, Nº4., Jul/Aug 2005.

Ichii, K., Fujimura, K. and Takase, T., 1986 "Structure of the ion-nitrided layer of 18-8 stainless steel", Tech. Rep. Kansai Univ.Vol. 27 pp. 135–144.

Isfahany, N.A.; Saghafian, H.; Borhani, G. The effect of heat treatment on mechanical properties and corrosion behavior of AISI420 martensitic stainless steel. Journal of Alloys and Compounds 509 (2011) 3931–3936

Kim, S.K., Yoo, J.S., Preiest, J.M. and Fewell, M.P., 2003, "Characteristics of martensitic stainless steel nitrided in a low pressure RF plasma", *Surface and Coatings Technology*, pp. 163–164, pp. 380–385

Li, C.X. and Bell, T., 2004, Corrosion properties of active screen plasma nitrided 316 austenitic stainless steel. Corrosion Science Vol. 46 pp. 1527 – 1547

Menthe, E., Rie, K.T., Schultze, J.W. and Simson, S., 1995, Structure and properties of plasma-nitrided stainless steel, Surface &. Coatings. Technology. Vol. 74–75 pp. 412–416.

Pinedo, C.E. and Monteiro, W.A., 2004, On the kinetics of plasma nitriding a martensitic stainless steel type AISI 420. Surface and Coatings Technology Vol. 179, pp. 119–123.

Xi, Y.T., Liu, D.X. and Han, D., 2008 "Improvement of corrosion and wear resistances of AISI 420 martensitic stainless steel using plasma nitriding at low temperature". Surface & Coatings Technology Vol. 202, pp. 2577–2583.

Xi, Y.T., Liu,D.X., Han, D., Han, Z.F., Improvement of mechanical properties of martensitic stainless steel by plasma nitriding at low temperature. Acta Metallurgica Sinica, (Engl. Lett.), Vol.21, Nº1, pp21-29 Feb. 2008

Zhang, Z.L. and Bell, T., 1985 "Structure and corrosion resistance of plasma nitrided stainless steel", Surface Engineering. Vol 1 pp. 131–136.

7. RESPONSIBILITY NOTICE

The authors are the only responsible for the printed material included in this paper.